Bowl-shaped ZnO ultrasonic transducer for photoacoustic/ultrasonic multimode microscopy

J. Zhang, D. Zhao, D. Li, F. Tian, Wei-Jiang Xu, X. Wu

Bowl-shaped ZnO ultrasonic transducer for photoacoustic/ultrasonic multimode microscopy

Jinying Zhang[#*]

School of Optics and Photonics, Beijing Key Laboratory for Precision Optoelectronic Measurement Instrument and Technology, Beijing Institute of Technology, Beijing, China
Institute of Semiconductors, Chinese Academy of Sciences, Beijing, China
[*]Corresponding author's email: jyzhang@bit.edu.cn

Dongdong Zhao[#]

School of Optics and Photonics, Beijing Key Laboratory for Precision Optoelectronic Measurement Instrument and Technology, Beijing Institute of Technology, Beijing, China
[#]Co-first author's email: 3220190480@bit.edu.cn

Defang Li

School of Optics and Photonics, Beijing Key Laboratory for Precision Optoelectronic Measurement Instrument and Technology, Beijing Institute of Technology, Beijing, China
Email: 3120195347@bit.edu.cn

Fengshuo Tian

School of Optics and Photonics, Beijing Key Laboratory for Precision Optoelectronic Measurement Instrument and Technology, Beijing Institute of Technology, Beijing, China
Email: 3220180407@bit.edu.cn

Weijiang Xu[*]

INSA Hauts-de-France, Université Polytechnique Hauts-deFrance CNRS, Univ. Lille, YNCREA, Centrale Lille, UMR 8520 IEMN-DOAE, Valenciennes, France
[*]Co-corresponding author's email: wei-jiang.xu@uphf.fr

Xianmei Wu

Institute of Acoustics, Chinese Academy of Sciences, Beijing, China
University of Chinese Academy of Sciences, Beijing, China
Email: wuxm@mail.ioa.ac.cn

***Abstract*—A bowl-shaped ultrasonic transducer is proposed for photoacoustic/ultrasonic multimode microscopy. The transducer uses zinc oxide (ZnO) as the piezoelectric material, which has a better electromechanical coefficient than flexible PVDF polymer and ensures the detection sensitivity. The ZnO film is spherically curved realizing self-focusing. It does not require an acoustic lens, consequently avoiding echo interference by the lens. In addition, it can be integrated with optical fibers. The resonant modes of the bowl-shaped ZnO film were calculated using finite element method. A photoacoustic/ultrasonic dual-modality imaging system is under development to adapt to the designed photoacoustic transducer. First test and imaging are carried out using a commercial ultrasonic transducer.**

Keywords—Bowl-shaped ultrasonic transducer, Self-focusing, ZnO, Dual-modality imaging

I. INTRODUCTION

In recent years, with the rapid development of image processing algorithms and computer technology, the medical imaging technology has gained dramatic progress. The main clinical imaging technologies include ultrasonic imaging technology [1-2], optical coherence tomography (OCT) technology [3-4], MRI technology [5-6], photoacoustic imaging technology [7-9], etc. These medical imaging technologies have their own advantages and disadvantages, and a single imaging technology can no longer meet the needs in applications. Therefore, medical imaging is currently changing toward multimodality and integration.

A multimode high-resolution imaging technology, photoacoustic (PA) imaging combining with optics and ultrasonics, has attracted significant attention due to its advantages of no-labeling, none destructive, irradiation-free, high-resolution [10], as well as superior depth-penetration [11] compared with OCT in biomedical detection [12-18]. This imaging technique is currently implemented in two main ways. The first one achieves the photoacoustic/ultrasonic combination by tilting the optical probe or the acoustic probe [15-17]. However, this approach limits the imaging depth of the system due to the non-coaxiality of the pulsed laser and ultrasound and the combined probe suffers from their bulky size. The second way tries to use a hollow acoustic probe to achieve confocal and coaxial properties of the pulsed laser and ultrasound [18-20]. K. Kirk Shung and Q. F. Zhou et al. [19] developed a hollow high-frequency ultrasonic transducer incorporating an acoustic focusing lens to improve sensitivity. Johannes Rebling et al. [20] prepared a ring-shaped high-frequency ultrasonic transducer using flexible material of PVDF. However, due to the low electromechanical coupling coefficient of PVDF polymer, the insertion of an acoustic lens between the piezoelectric transducer and the detection medium causes echo interference and acoustic energy loss, which reduces the imaging performance of the ultrasonic transducer. To solve this problem, a bowl-shaped ZnO ultrasonic transducer for PA application is proposed in this paper.

The bowl-shaped ultrasonic transducer is designed and modeled using finite element method (FEM). To understand the performance of the transducer, the resonant modes and acoustic fields of a planar ZnO film, a curved ZnO film, a bowl-shaped (with a central hole of optical fiber diameter) ZnO film, and a bowl-shaped PVDF film are first simulated. By optimizing the dimension of the ZnO film, the thickness resonant mode without coupling with other parasite modes is obtained. Secondly, the acoustic field generated by the vibration of the bowl-shaped ZnO film and the curved ZnO film is compared with that of the planar ZnO film to show that the acoustic energy loss due to the open hole in the bowl-shaped ZnO film is minus and does not affect the focusing property of the transducer. Meanwhile, the (pressure field?) intensity of the bowl-shaped ZnO film is much larger than that of the bowl-shaped PVDF film. Finnaly, a photoacoustic/ultrasonic dual-modality imaging system under construction is described.

This work was supported by National Key Research and Development Program of China (2018YFF01010304, 2018AAA0100301), and National Natural Science Foundation of China (No. 62174012, 61704166).

II. Configuration

Thin sheet-shaped piezoelectric vibrators (rectangular sheets, circular sheets, rings, etc.) are polarized along the thickness direction which is also their vibration direction. The characteristics of this vibration are related to the electromechanical coupling coefficient k_t. The k_t value of ZnO is much larger than that of PVDF. The vibration of thickness-stretching requires the diameter of the vibrator to be 10 times larger than the thickness. When a plane wave transmission is required, this ratio should be 50 times larger to avoid the interference of the resonance with other complex vibration modes. Theoretically, the resonant frequency of the thickness-stretching vibration is determined by:

$$f=c/2t \qquad (1)$$

where f is the resonant frequency, c the wave speed in the piezoelectric sheet, and t the thickness of the sheet.

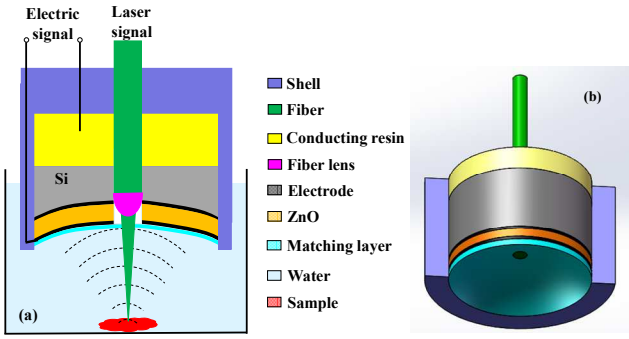

Fig. 1 Structure of the bowl-shaped ultrasonic transducer: (a) two-dimensional schematic diagram of photoacoustic/ultrasonic dual-modality imaging; (b) three-dimensional diagram.

Fig.1 shows the proposed bowl-shaped ultrasonic transducer, which bends the piezoelectric film itself to achieve beam focusing instead of by using an acoustic focusing lens and thus avoiding multiple reflection interference of the waves in the lens. A hollow hole is designed in the center of the curved piezoelectric film so that an optical fiber probe can be directly integrated with the acoustic transducer to make them coaxial and confocal. The aperture of the hollow hole is set to 200 μm based on the actual self-focusing fiber size.

III. Simulation Results and Discussion

As the resonant frequency is determined by the thickness of the piezoelectric film, the resonant modes of two groups of planar and curved ZnO films of different diameter are calculated with the same thickness of 43 μm. The first group has a diameter of 1 mm, and the other group has a diameter of 5 mm. In FEM simulation, the surface boundaries of the films are mechanically free and the film extremities are fixed. As shown in Figs. 2a and 2c, for film diameter of 1 mm, there are significant parasite vibration modes superposed to or near the resonance mode, while in Figs. 2b and 2d, for film diameter of 5 mm, the parasite modes are not presented. Such parasite modes can also be identified from their electric impedance curves as calculated in Fig. 3.

The resonant frequencies of the two groups of piezoelectric film can be evaluated from the electric impedance curves. For the group they are both 73.8 MHz (Figs. 3a and 3b). For the second group, the resonant frequency of the curved ZnO film is 73.5 MHz and that of the planar ZnO film is 74.0 MHz. These simulated resonant frequencies based on FEM are in good agreement with the theoretical values of Eq. (1).

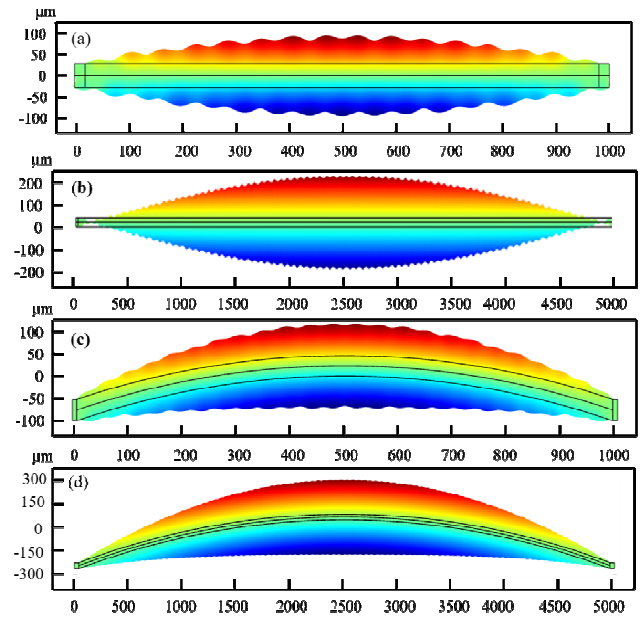

Fig. 2 Resonant modes of ZnO thin film piezoelectric: (a) planar ZnO thin film piezoelectric sheet with 1 mm length; (b) planar ZnO thin film piezoelectric sheet with 5 mm length; (c) curved ZnO thin film piezoelectric sheet with 1 mm length; (d) curved ZnO thin film piezoelectric sheet with 5 mm length.

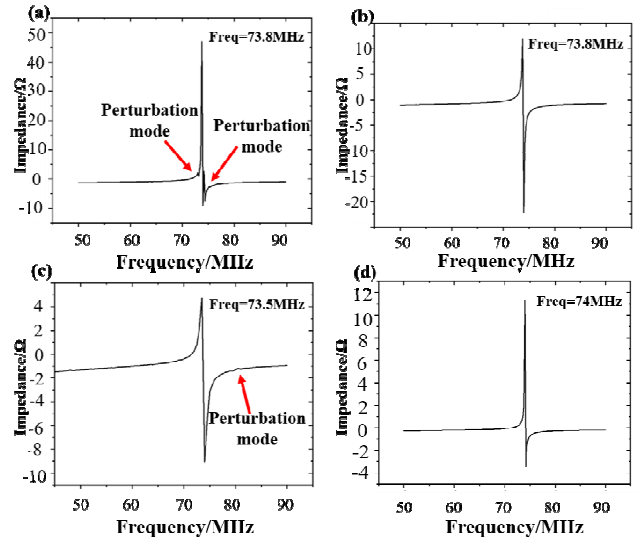

Fig. 3 Electrical impedance curves of ZnO piezoelectric film: (a) planar ZnO sheet of 1 mm diameter; (b) curved ZnO sheet of 1 mm diameter; (c) planar ZnO sheet of 5 mm diameter; (d) curved ZnO sheet of 5 mm diameter.

To compare the transducer performance of different configurations and with different piezo-materials, four types of piezoelectric transducers, including those of backing planar ZnO films, curved ZnO films, bowl-shaped ZnO films and bowl-shaped PVDF films, are analyzedThe acoustic field distribution in water are calculated. The thickness of the ZnO film is still set to be 43 μm for an operating frequency of about 70 MHz. Since the acoustic wave speed in PVDF is different from that of ZnO, the thickness of PVDF film is set to be 23 μm according to Eq. (1). Fig. 4 shows the acoustic field (pressure) distribution

in water for each transducer emitting ultrasound in their thickness vibration mode. Both the curved and the bowl-shaped films have a desired focusing. From Fig. 4a, the field focused by the conventional planar ZnO film with acoustic lens has a more important sidelobe than those with the curved film and the bowl-shaped film.

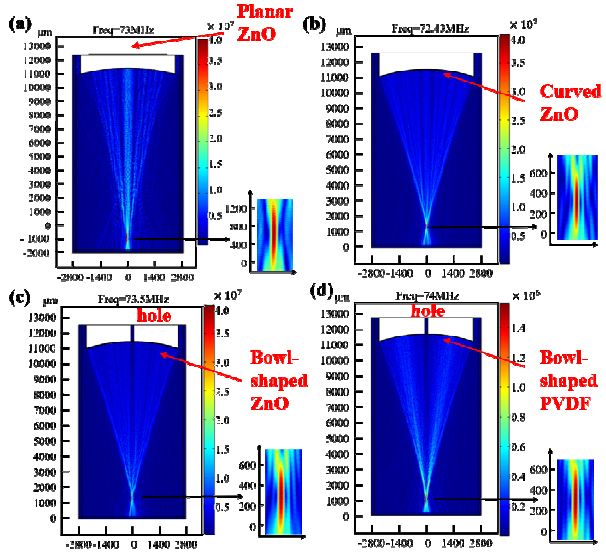

Fig. 4 Acoustic field distribution (in water) of different piezoelectric transducers with: (a) planar ZnO film; (b) curved ZnO film; (c) bowl-shaped ZnO film; (d) bowl-shaped PVDF film.

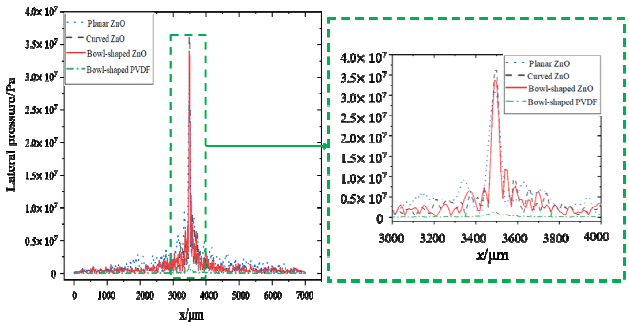

Fig. 5 Lateral pressure (in magnitude) of the piezoelectric transducers in water.

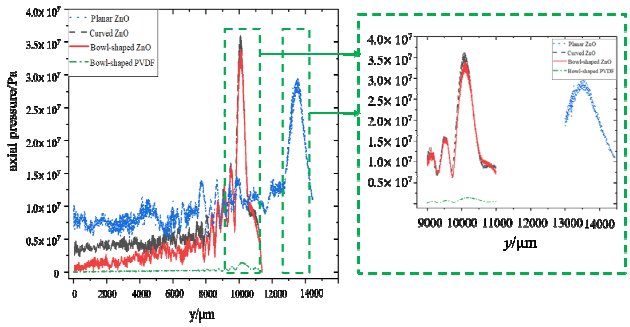

Fig. 6 Axial pressure (in magnitude) of the piezoelectric transducers in water.

Fig. 5 and Fig. 6 display the comparison of the numerical simulation results of the lateral and the axial pressure distribution in water for the four types of the transducers. First, the acoustic pressure at the focal point for the transducer of the curved ZnO film is larger than that of the planar ZnO film. This is due to that the curved ZnO film is self-focused and avoids the acoustic energy loss caused by the multiple reflection in the acoustic focusing lens. Second, although the bowl-shaped ZnO film has a slight energy loss due to a hollow hole compared to the curved one, its acoustic pressure is still larger than that of the planar one. Third, since the piezoelectric coefficient of ZnO is much higher than that of PVDF, the acoustic pressure of the transducer with the bowl-shaped ZnO film is 20 times higher than that of the bowl-shaped PVDF film. In summary, the bowl-shaped ZnO transducer has desired emission intensity as well as detection sensitivity. Its hollow configuration ensures convenient integration with an optical fiber lens. Therefore, it is a promising candidate in photoacoustic/ultrasonic dual-modality imaging.

Ⅳ. Experiments

Fig. 7 shows the photoacoustic/ultrasonic dual-modality imaging system. The optical signal is provided by a 532 nm pulsed laser with a pulse width of 2 ns and a repetition frequency of 4 kHz, and then coupled through the objective lens into a 460-HP single-mode fiber with a mode field diameter of 3.5 μm and a numerical aperture of 0.13. The optical beam is focused by the microscopic objective lens at the surface of the detecting object. The spot size after focusing is within 10 μm. The ultrasonic transducer and microscope objective are mounted and fixed to a mechanical arm which is driven by the stepper motor to perform two-dimensional (2D) scanning for three-dimensional imaging. The ultrasonic transducer is excited by a pulser-receiver (JSR500). An oscilloscope (RTB2000) is used as data acquisition system to acquire the ultrasonic data. Actually, a commercial ultrasonic focusing transducer of 70 MHz working frequency is used to test the imaging system. Fig. 7 shows the ultrasonic imaging results of a coin sample. And different outline images of the sample are generated through different imaging algorithms.

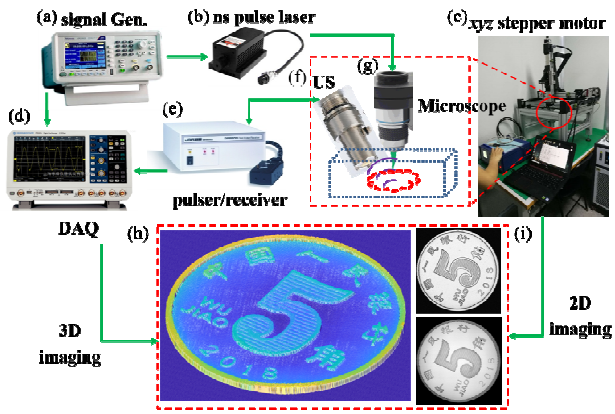

Fig. 7 The built photoacoustic/ultrasonic dual-modality imaging system: (a) signal generator; (b) 532 nm laser; (c) triaxial displacement stage; (d) oscilloscope; (e) pulser-receiver; (f) ultrasonic transducer; (g) microscope objective; (h) 3D image of the coin; (i) 2D image of the coin.

We test the performance of a commercial planar ultrasonic transducer using this photoacoustic/ultrasonic dual-modality imaging system. At first, the transducer is moved along *z*-axis to find the focal point. To get a high signal-to noise ratio of the pulse echo, the coin sample is placed at the focal plane. The pulse echo was recorded by an oscilloscope. The echo data are filtered and Fourier transformed to obtain the echo spectrum of the ultrasonic transducer, as shown in Fig. 8. We can see that the center

frequency of the ultrasonic transducer is 70 MHz and the 3 dB bandwidth is 60 MHz, which coincides with the manufacturer's calibration value. This commercial ultrasonic transducer does not have a hollow hole at the center, and it is difficult to be integrated with the optical objective coaxially. The photoacoustic imaging has not been performed. Next work will include the preparation of the bowl-shaped ultrasonic transducer and the coaxial photoacoustic imaging.

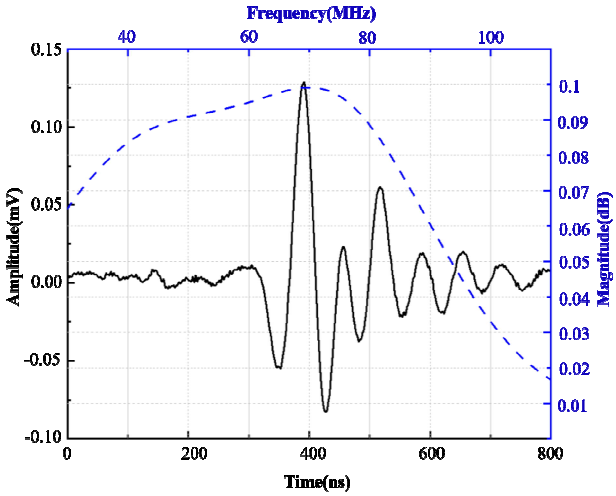

Fig. 8 Pulse-echo signal testing and spectrum analysis of the transducer

CONCLUSION

We propose a new bowl-shaped ultrasonic transducer. Compared to planar and curved piezoelectric films, this bowl-shaped ultrasonic transducer exhibits superior energy intensity and no multiple reflection interference. Different piezoelectric materials, ZnO and PVDF are also compared. The bowl-shaped ultrasonic transducer has confocal and coaxial characteristics for pulsed laser and ultrasonic waves, which meets the requirements of photoacoustic/ultrasonic dual-modality imaging. A photoacoustic/ultrasonic imaging system is under built and successfully used to image objects and test the pulse-echo signal of the ultrasonic transducer. Next step will focus on the preparation of this new bowl-shaped ultrasonic transducer and to test its performance using our imaging system. By integrating the self-focusing fiber with the bowl-shaped ultrasonic transducer, the detection sensitivity of the photoacoustic/ultrasonic dual-modality imaging system would be improved and the probe can be significantly miniaturized.

REFERENCES

[1] Hofman T, Raum K, Leguerney I, et al. Assessment of bone structure and acoustic impedance in C3H and BL6 mice using high resolution scanning acoustic microscopy [J]. Ultrasonics, 44,1307-1311(2006).

[2] Wu J, Pepe J, Rincón M. Sonoporation, anti-cancer drug and antibody delivery using ultrasound [J]. Ultrasonics, 44,21-25(2006).

[3] Shi C, Wang M, Zhu T, et al. Machine learning helps improve diagnostic ability of subclinical keratoconus using Scheimpflug and OCT imaging modalities [J]. Eye and Vision, 7(1): 48(2020).

[4] Zeng Y, Xu S, Chapman W C, et al. Real-time colorectal cancer diagnosis using PR-OCT with deep learning; proceedings of the Biophotonics Congress: Biomedical Optics , [C] (2020).

[5] Wang S, Lin R, Cheng S, et al. Assessment of Water Mobility in Surf Clam and Soy Protein System during Gelation Using LF-NMR Technique [J]. Foods, 9(2) (2020).

[6] Sharma M K, Shah R P, Sengupta P. Amalgamation of stress degradation and metabolite profiling in rat urine and feces for characterization of oxidative metabolites of flibanserin using UHPLC-Q-TOF-MS/MS, H/D exchange and NMR technique [J]. Journal of Chromatography B, 1139,21993(2020).

[7] Zlitni A, Gowrishankar G, Steinberg I, et al. Maltotriose-based probes for fluorescence and photoacoustic imaging of bacterial infections [J]. Nature Communications , 11(1): 1250(2020).

[8] Yang C, Lan H, Gao F, et al. Review of deep learning for photoacoustic imaging [J]. Photoacoustics, 21,100215(2021).

[9] Das D, Sharma A, Rajendran P, et al. Another decade of photoacoustic imaging [J]. Physics in Medicine & Biology, 66(5): 05TR1(2021).

[10] Zhou J, Jokerst J V. Photoacoustic imaging with fiber optic technology: A review [J]. Photoacoustics, 20,100211(2020).

[11] Christensen-Jeffries K, Couture O, Dayton P A, et al. Super-resolution Ultrasound Imaging [J]. Ultrasound in Medicine & Biology, 46(4): 865-891(2020).

[12] Daoudi K, Van Den Berg P J, RABOT O, et al. Handheld probe integrating laser diode and ultrasound transducer array for ultrasound/photoacoustic dual modality imaging [J]. Opt Express, 22(21): 26365-26374(2014).

[13] Mallidi S, Watanabe K, Timerman D, et al. Prediction of tumor recurrence and therapy monitoring using ultrasound-guided photoacoustic imaging [J]. Theranostics, 5(3): 289-301(2015).

[14] Park E-Y, Park S, Lee H, et al. Simultaneous Dual-Modal Multispectral Photoacoustic and Ultrasound Macroscopy for Three-Dimensional Whole-Body Imaging of Small Animals [J]. Photonics, 8(1),(2021).

[15] Wang C, Guo L, Wang G, et al. In-vivo imaging of melanoma with simultaneous dual-wavelength acoustic-resolution-based photoacoustic/ultrasound microscopy [J]. Appl Opt, 2021, 60(13): 3772-3778(2021).

[16] Yang M, Zhao L, He X, et al. Photoacoustic/ultrasound dual imaging of human thyroid cancers: an initial clinical study [J]. Biomed Opt Express, 8(7): 3449-3457(2017).

[17] Todd N E, Alejandro G-U, Arie K, et al. A dual-modality photoacoustic and ultrasound imaging system for noninvasive sentinel lymph node detection: preliminary clinical results; proceedings of the ProcSPIE, F, 2014 [C] .

[18] Yang J-M, Favazza C, CHEN R, et al. Simultaneous functional photoacoustic and ultrasonic endoscopy of internal organs in vivo [J]. Nature Medicine, 18(8): 1297-1302(2012).

[19] Yang J-M, Chen R, Favazza C, et al. A 2.5-mm diameter probe for photoacoustic and ultrasonic endoscopy [J]. Opt Express, 20(21): 23944-23953(2012).

[20] Rebling J, Estrada H, Gottschalk S, et al. Dual-wavelength hybrid optoacoustic-ultrasound biomicroscopy for functional imaging of large-scale cerebral vascular networks [J]. Journal of Biophotonics, 11(9): e201800057(2018).